A Compact and Low-Profile High-Gain Multilayer Vivaldi Antenna Based on Gradient Metasurface Superstrates

Ababil Hossain, Stephen Pancrazio, Tyler Kelley, and Anh-Vu Pham, *fellow, IEEE*

***Abstract*— This letter presents the design, analysis, and implementation of an electrically compact high-gain multilayer Vivaldi antenna. The multilayer antenna comprises gradient metasurface superstrate layers arranged on the top and bottom of a central electrically compact Vivaldi antenna via low-loss polyethylene foam spacers. The overall electrical dimensions of the antenna are $0.36\lambda_0$ x $0.29\lambda_0$ x $0.06\lambda_0$, covering a bandwidth from 450 MHz to 10 GHz with an average measured forward gain of more than 15 dBi (λ_0: free space wavelength at 450 MHz). The unit pixel dimensions of the gradient metasurface layer have been optimized to achieve a high-flat gain profile within the desired bandwidth of the antenna. The metasurface layers are printed on thin Kapton polyimide boards to minimize the system's weight. The prototyped antenna is extremely low-profile and weighs 182 grams, making it ideally suited for lightweight UWB applications needing a very high forward gain.**

***Index Terms*— Multilayer Vivaldi antenna, high-gain antenna, compact antenna, lightweight antenna, gradient metasurface.**

I. INTRODUCTION

Compact and lightweight antennas are important for UAV (Unmanned Aerial Vehicle) radar imaging systems for increased fuel and space efficiency. At the same time, radar antennas need to be ultrawideband and high gain for enhanced imaging resolution [1, 2]. However, fundamental limitations make it difficult to design compact antennas with high-gain and wide-bandwidth performance [3-5]. While Vivaldi-type end-fire antennas are often used for radar applications, their compact counterparts exhibit lower gain due to a small aperture area [6, 7]. To overcome this limitation, a few innovative designs have been proposed based on enhancing localized current density in the electrically compact aperture to increase the radiated power. Among these, tapered slots and cavity structures have been deployed in Vivaldi antennas to boost the gain [8-10]. Furthermore, metamaterials or dielectric directors have been used in Vivaldi for gain enhancement, especially at higher frequencies [11-14]. Yet, these gain enhancement techniques are narrowband mainly due to the resonant nature of the metamaterials and tend to increase the antenna's size and weight.

Multilayer designs offer the possibility of further gain enhancement without increasing the lateral dimension of the antenna. In a Vivaldi antenna, a multi-layer design can channel the spurious radiation into forward-propagating surface waves to enhance the forward gain without increasing the overall lateral dimension. In this regard, a few 3-D multilayer Vivaldi antenna designs incorporating homogenous metamaterial superstrates have been demonstrated to improve gain by around 4-6 dB [15-17]. However, the major issue with these designs is that the gain flatness decreases drastically at higher frequencies, negatively affecting the antenna's usable gain bandwidth. The gain drop happens due to pattern distortion at higher frequencies caused by the dispersion of the phase front of the propagating surface waves within the metamaterial superstrates. Similarly, multilayer designs employing dielectric superstrates can concentrate stronger electric fields for surface wave propagation and thus increase the gain [18- 20]. Nevertheless, the gain enhancement is insufficient, and the gain flatness worsens due to phase dispersion similar to the homogenous metamaterial or metasurface case. Lastly, the reported multi-layer antennas leveraging homogenous metamaterial or dielectric superstrate deploy an electrically larger central Vivaldi antenna [15-20], resulting in a larger dimension and higher overall weight for the whole system.

In this letter, we present an electrically compact high-gain multilayer Vivaldi antenna based on the new gradient metasurface superstrate concept. By gradient modulation of the length of the metasurface's unit cell, the overall gain profile of the antenna has been increased to a broader bandwidth. Low-weight polyethylene foam spacers are used to attach the metasurface layers to the compact Vivaldi antenna [10], which is the central antenna. This makes the overall antenna structure electrically very compact ($0.36\lambda_0$ x $0.29\lambda_0$ x $0.06\lambda_0$) and lightweight (182 grams), covering a bandwidth from 450 MHz to 10 GHz with an average forward gain of 15.37 dBi.

II. ANTENNA GEOMETRY, FABRICATION AND WORKING MECHANISM

A. Overview of the Antenna Structure

The multilayer antenna design is displayed in the schematic diagram of Fig. 1. The main dimensional specifications with numerical values of the structure are given in Table I. The multilayer antenna structure consists of three major parts: central Vivaldi [10], gradient metasurface layers, and low-loss

This project is sponsored by the Department of the Navy, Office of Naval Research under award N00014-22-1-2167. Any opinions, findings, and conclusions ore recommendations expressed in this material are those of author(s) and do not necessarily reflect the views of the Office of Naval Research. (Corresponding author: Ababil Hossain)

lightweight polyethylene foam spacers for mechanical support.

a) Central Vivaldi Antenna

For the central antenna, a cavity-based electrically compact and high-gain Vivaldi radiator has been used [10]. Cascaded cavity-based substrate cut-out in the original Vivaldi causes 40% size miniaturization, 2-3 dB low-frequency gain enhancement, and 20% reduction in overall weight. The Vivaldi antenna measures 24.4 cm × 19.5 cm in lateral dimensions and weighs only 151 grams. It covers a bandwidth of 450 MHz-10 GHz with an average forward realized gain of 10.82 dBi.

b) Gradient Metasurface Layers

Gradient metasurface layers composed of rectangular metallic pixels have been used as superstrates. They are placed on the top and bottom of the central Vivaldi antenna and are denoted by MS-1 and MS-2 respectively in Fig. 1. The metallic pixels are printed on a 50-µm thin Kapton polyimide board to reduce the system's overall weight. The metasurface layer is symmetric about the center (YZ plane). The width and inter-pixel gap of the unit pixel are optimized to be 2 mm and 0.8 mm, respectively. However, the length of the unit pixel gradually decreases from the center to the edge from 6 mm to 2 mm in pixel type A to type E.

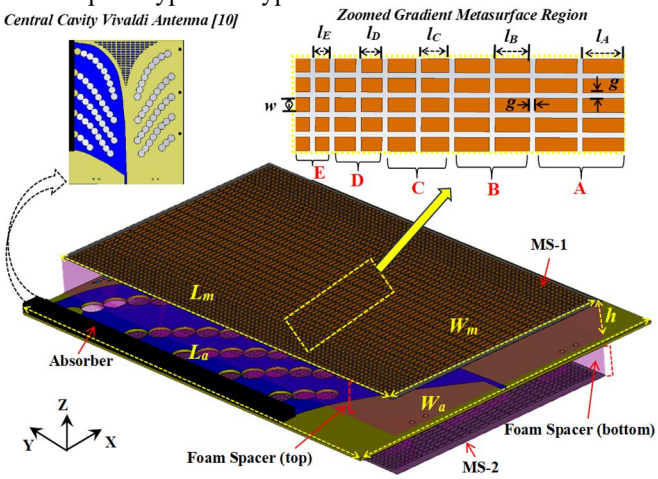

Fig. 1. 3-D schematic diagram of the multilayer Vivaldi antenna. (*For the better visibility of the metasurface layers, foam spacers are made transparent in pink color*)

TABLE I
GEOMETRICAL PARAMETERS OF THE OPTIMIZED ANTENNA

Parameter	Value (mm)	Parameter	Value (mm)
L_a	244	l_C	4
W_a	195	l_D	3
L_m	240	l_E	2
W_m	140	w	2
l_A	6	g	0.8
l_B	5	h	19.05

c) Polyethylene Foam Spacers

Low-loss (ϵ_r=1.2, tanδ=0.0005) and lightweight (0.03 gm/cm^3) polyethylene foam spacers are chosen for the mechanical support of the metasurface layers. Foam thickness is 0.75″ (19.05 mm), approximately half-wavelength at 6 GHz (roughly middle of the operating band 0.45-10 GHz).

B. Fabrication Cycle and Multilayer Assembly

The central Vivaldi antenna built on a Rogers5880 substrate is sandwiched between polyethylene foam spacers. Two metasurface polyimide layers are then glued on the top and bottom foam layers to complete the assembly process. The assembled multilayer antenna measures 9.5″×7.6″×1.5″. The fabrication cycle of the antenna is shown in Fig. 2.

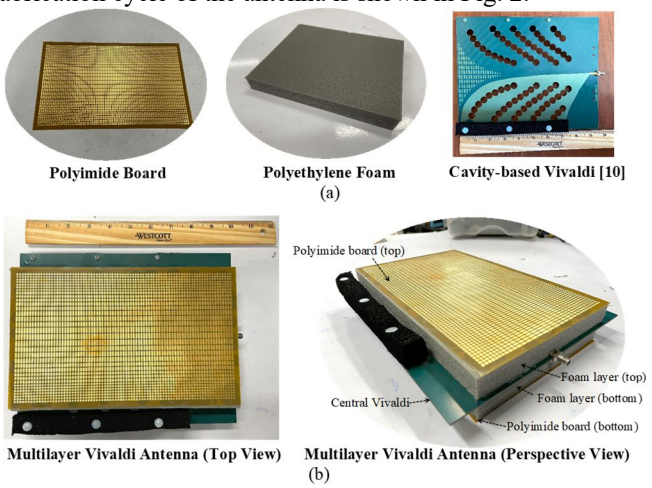

Fig. 2. Fabrication cycle and prototyping of multilayer Vivaldi. (a) Assembly components (b) Assembled Antenna.

C. Theory and Working Principle

The radiation mechanism of the antenna is explained in Fig. 3. The Vivaldi, along with metasurface layers, functions as a composite structure contributing to multilayered radiation. In a typical Vivaldi, traveling waves are radiated at higher frequencies in the end-fire direction from the tapered microstrip to the slot line transition. However, some out-of-end-fire field leakage causes spurious sidelobes in the pattern, reducing the forward or end-fire gain, as shown in Fig. 3(a). Metasurface superstrate layers can guide this spurious plane wave radiation towards the end-fire direction, enabling a significant gain enhancement [21] as in Fig. 3(b). In the multilayer antenna, E_s^t and E_s^b are the electric fields of the propagating surface waves, and E_0 is the electric field of the original central Vivaldi. Metal strips with gradient widths and gaps have been successfully used as a cover for narrowband SIW leaky wave antennas, showing a gain increase of 4-6 dBi [22]. However, because of its wider bandwidth and end-fire characteristics, the Vivaldi type antenna needs a broadband metasurface cover to channel the incidence surface waves toward its endfire direction.

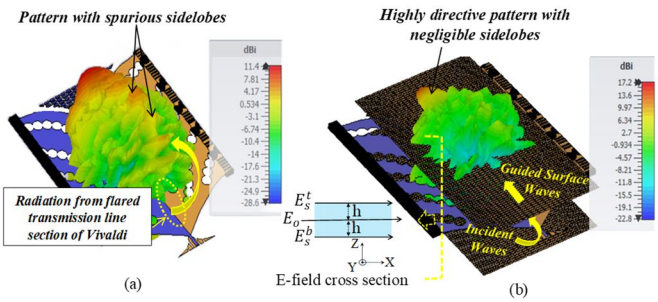

Fig. 3. Illustration of radiation phenomena. (a) Original single Vivaldi and (b) Multilayer Vivaldi with patterns at 10 GHz.

The patterned metasurface structures exhibit slow-wave and fast-wave characteristics depending on the frequencies of the incident plane waves [23]. The unit pixel dimensions of the metasurface are optimized so that the transition between the slow-wave and fast-wave mode occurs outside the band of operation of the antenna. At lower frequencies (<10 GHz in our design), the slow-wave mode dominates in the metasurface region, which confines a strong localized electric field for the propagating surface waves, causing significant gain enhancement as shown in Fig. 3(b). After 10 GHz, fast-wave mode gradually dominates causing undesirable out-of-end-fire leaky wave radiation.

In Fig. 4, the gain and return loss profile is compared among different layer versions of the antenna. It's evident that the gain increases gradually with each additional layer. With gradient metasurface as superstrates, gain increases gradually from 2 GHz when the traveling wave mode radiation of the central Vivaldi starts to dominate. With the increase in frequency, the electrical length of the metasurface layer increases proportionally, which causes the gain to increase gradually up to 10 GHz. Noticeably, the metasurface layers have a negligible impact on the gain below 2 GHz. This is because the Vivaldi mainly functions as a resonant antenna at lower frequencies, where its near-field pattern possesses a significant portion of the perpendicular E-field component. Hence, the pixelated metasurface layer remains almost transparent to EM fields emanating from the central Vivaldi, without affecting the antenna's overall gain performance. From the return loss (S_{11}) parameter, it is also seen that due to the impedance transformation of the metasurface layer matching improves and unwanted ripples in return loss are mitigated at several higher frequencies near 9 GHz in the multilayer antenna.

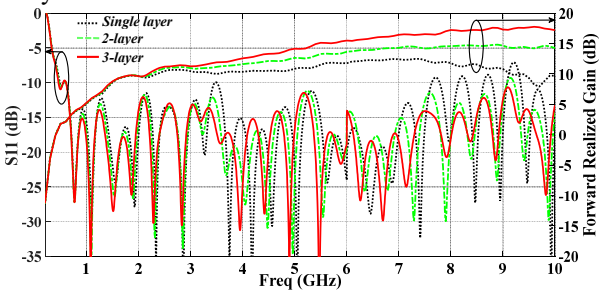

Fig. 4. Simulated S_{11} and gain comparison (Single layer: only Vivaldi; 2-layer: Vivaldi with one metasurface; 3-layer: Vivaldi with two metasurfaces)

III. Optimization Of The Metasurface Layers

a) Gradient versus Homogenous Metasurface Layers

The main challenge with this type of multilayer gain enhancement scheme is maintaining an undistorted phase-front of the propagating surface waves on the metasurface. With a homogenous metasurface layer, the wavefront starts to split into multiple waves at higher frequencies due to spatial dispersion decreasing the forward gain [24]. Gradient metasurface transforms the phase-front of the propagating surface wave at higher frequencies [25]. As shown in Fig. 5(a), the length of the metasurface unit cell is decreased symmetrically from the center towards the edge to create a variable phase gradient along the direction transverse to the propagation. By decreasing the length of unit pixels, the metasurface portion becomes less inductive and the value of the transverse component of the phase constant gradually decreases from the center towards the edge, making $|\beta_E|$ .... < $|\beta_B|$< $|\beta_A|$. This compensates for the transmission phase difference causing dispersion that happens to a plane wave along the line transverse to the direction of propagation. Fig. 5(b) shows the dispersion curve depicting the slow-wave and fast-wave regions of the metasurface.

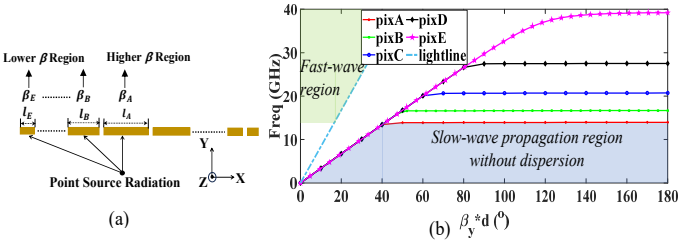

Fig. 5. (a) Schematic diagram showing low and high wavenumber ***(β)*** region in the gradient metasurface layer (b) dispersion curve ($\beta_y d$ versus frequency) for various pixel types (pixel A to E) using CST Eigen mode solver.

The phenomenon is illustrated in Fig. 6 with patterns at 10 GHz. As seen in Fig. 6(a), with the gradient metasurface, the phase front remains in a line yielding a highly directive end fire pattern. Whereas with homogenous metasurface consisting of 6 mm unit pixel length, the phase front gets distorted at higher frequencies when the superstrate height (h) exceeds half-wavelength at the midband (~6.4 GHz). This yields pattern with multiple lobes as in Fig. 6(b).

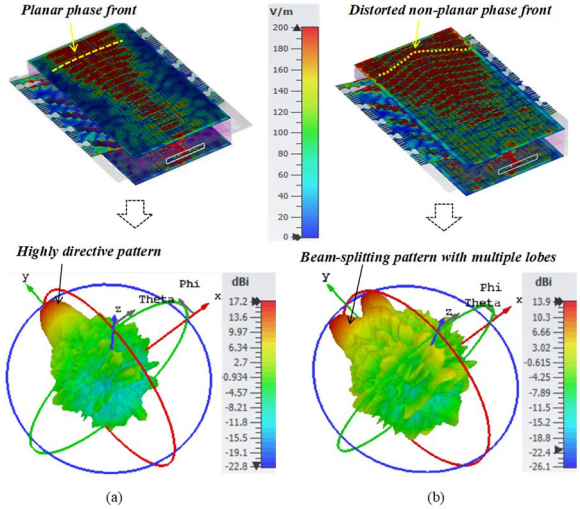

Fig. 6. Electric field distribution and corresponding radiation patterns at 10 GHz with (a) gradient and (b) homogenous metasurface superstrates.

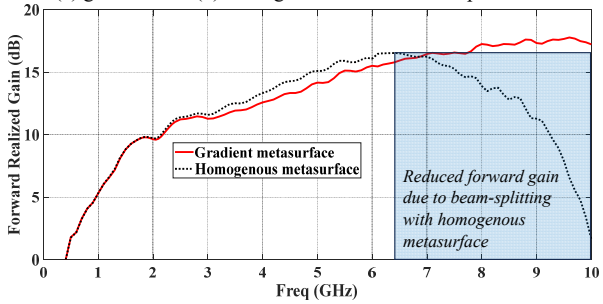

Fig. 7. Comparison of gain versus frequency with gradient and homogenous metasurface as superstrates in multilayer Vivaldi.

From the gain versus frequency plot in Fig. 7, it is seen that the beam-splitting causes a significant reduction in the forward gain of the antenna after 6.4 GHz with homogenous metasurface case. On the contrary, with optimized phase-gradient metasurface, the gain bandwidth can be extended and an enhanced gain up to 10 GHz can be attained.

b) Optimization of pixel gap (g) & metasurface heigh (h)

A smaller interpixel gap limits the usable gain bandwidth, while a higher gap broadens the gain bandwidth of the antenna shown in Fig. 8(a). The optimal interpixel gap for ensuring the antenna's operability up to 10 GHz is determined to be 0.8 mm. From Fig. 8(b), it is seen that both lower (12.7 mm) and higher (25.4 mm) superstrate heights lead to reduced gain. The multilayer antenna achieves optimal gain performance at a superstrate height of 19.05 mm (~0.45λ), where λ is the wavelength within the foam spacer medium near the mid-band frequency of 6.4 GHz.

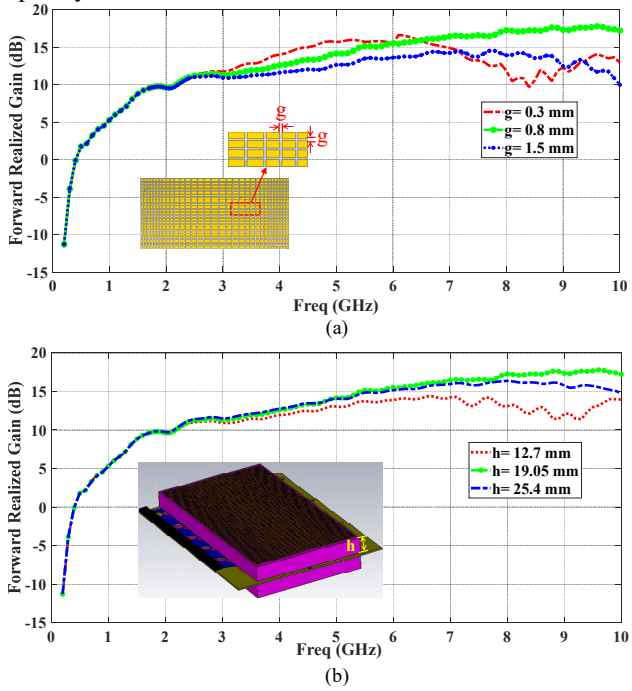

Fig. 8. Comparison of simulated gain versus frequency for (a) different inter-pixel gaps and (b) superstrate heights.

IV. Measurement Results

The radiation patterns, return loss, and gain of the multilayer Vivaldi antenna were measured and compared with the simulation. Fig. 9 shows the radiation pattern comparison of the multilayer Vivaldi, where it is seen that the measured 2-D patterns conform to the simulation satisfactorily in both E and H planes. Fig. 10 shows that the -10 dB S_{11} bandwidth of the antenna covers from 450 MHz to 10 GHz with an average forward realized gain exceeding 15 dBi. There is a small dip in the measured gain curve near 9.7 GHz, which is still within the acceptable limit. Table II compares the gain and bandwidth performance, where it is evident that the presented multilayer Vivaldi shows a superior gain and bandwidth ratio with relatively compact electrical dimensions compared to other similar antennas in the literature. For the average gain calculation, 10 data points excluding notches are considered.

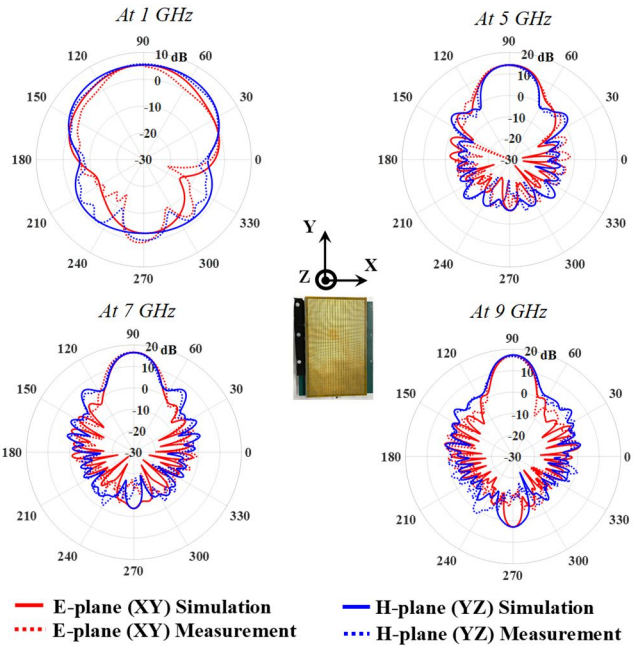

Fig. 9. Measured 2-D radiation patterns (realized gain) comparison of the multilayer Vivaldi antenna.

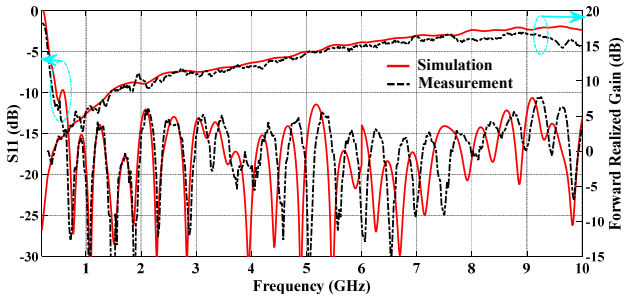

Fig. 10. Measured return loss and gain comparison of the multilayer Vivaldi Antenna.

TABLE II

COMPARISON OF MULTILAYER VIVALDIS IN LITERATURE

Ref. No	3D Electrical Dimensions	Impedance Bandwidth Ratio	Average Gain
[15]	$0.73\lambda_0 \times 0.49\lambda_0 \times 0.05\lambda_0$	11.8: 1	14.45 dB
[16]	$0.76\lambda_0 \times 0.48\lambda_0 \times 0.07\lambda_0$	11.6: 1	13.44 dB
[17]	$0.94\lambda_0 \times 0.61\lambda_0 \times 0.17\lambda_0$	4.6: 1	12.64 dB
[18]	$0.75\lambda_0 \times 0.61\lambda_0 \times 0.18\lambda_0$	4.71: 1	11.52 dB
[19]	$1.71\lambda_0 \times 0.92\lambda_0 \times 0.11\lambda_0$	11.9: 1	14.36 dB
[20]	$1.05\lambda_0 \times 0.61\lambda_0 \times 0.163\lambda_0$	4.71: 1	12.74 dB
This paper	*$0.36\lambda_0 \times 0.29\lambda_0 \times 0.06\lambda_0$*	*22.4: 1*	*15.37 dB*

V. Conclusion

This letter presents a novel approach based on gradient metasurface superstrates to enhance the gain profile of an electrically compact Vivaldi antenna. The 3-D antenna design consists of a central electrically compact Vivaldi antenna along with two pixelated phase-gradient metasurface superstrate layers supported by low-loss polyethylene foam spacers. The novel pixelated gradient metasurface concept overcomes the traditional limitation of usable gain bandwidth within a multilayer Vivaldi antenna.

REFERENCES

1. Allen, Ben, et al. "Ultra-wideband: Applications, technology and future perspectives." *international workshop on convergent technologies (IWCT)*, 2005.
2. Coburn, William, and Seth McCormick. "Ultra-wideband antenna performance comparison." *2018 International Applied Computational Electromagnetics Society Symposium (ACES)*. IEEE, 2018.
3. Wheeler, Harold A. "Fundamental limitations of small antennas." *Proceedings of the IRE* 35.12 (1947): 1479-1484.
4. Wheeler, Harold. "Small antennas." in *IEEE Transactions on antennas and propagation* 23.4 (1975): 462-46.
5. Harrington, Roger F. "Effect of antenna size on gain, bandwidth, and efficiency." *J. Res. Nat. Bur. Stand* 64.1 (1960): 1-12.
6. C. Deng and Y. -j. Xie, "Design of Resistive Loading Vivaldi Antenna," in *IEEE Antennas and Wireless Propagation Letters*, vol. 8, pp. 240-243, 2009.
7. S. Saleh, W. Ismail, I. S. Zainal Abidin, M. H. Jamaluddin, M. H. Bataineh and A. S. Al-Zoubi, "Novel Compact UWB Vivaldi Nonuniform Slot Antenna With Enhanced Bandwidth," in *IEEE Transactions on Antennas and Propagation*, vol. 70, no. 8, pp. 6592-6603, Aug. 2022.
8. P. Fei, Y. Jiao, W. Hu and F. Zhang, "A Miniaturized Antipodal Vivaldi Antenna With Improved Radiation Characteristics," in *IEEE Antennas and Wireless Propagation Letters*, vol. 10, pp. 127-130, 2011.
9. R. Natarajan, J. V. George, M. Kanagasabai and A. Kumar Shrivastav, "A Compact Antipodal Vivaldi Antenna for UWB Applications," in *IEEE Antennas and Wireless Propagation Letters*, vol. 14, pp. 1557-1560, 2015.
10. A. Hossain and A. -V. Pham, "A Novel Gain-Enhanced Miniaturized and Lightweight Vivaldi Antenna," in *IEEE Transactions on Antennas and Propagation*, vol. 71, no. 12, pp. 9431-9439, Dec. 2023.
11. B. Zhou and T. J. Cui, "Directivity Enhancement to Vivaldi Antennas Using Compactly Anisotropic Zero-Index Metamaterials," in *IEEE Antennas and Wireless Propagation Letters*, vol. 10, pp. 326-329, 2011.
12. Deng, RC., Yang, Xm., Ma, B. et al. Performance enhancement of novel antipodal Vivaldi antenna with irregular spacing distance slots and modified-w-shaped metamaterial loading. *Appl. Phys. A* 125, 5 (2019).
13. Bourqui, M. Okoniewski and E. C. Fear, "Balanced Antipodal Vivaldi Antenna With Dielectric Director for Near-Field Microwave Imaging," in *IEEE Transactions on Antennas and Propagation*, vol. 58, no. 7, pp. 2318-2326, July 2010.
14. R. Cicchetti, V. Cicchetti, A. Faraone, L. Foged and O. Testa, "A Compact High-Gain Wideband Lens Vivaldi Antenna for Wireless Communications and Through-the-Wall Imaging," in *IEEE Transactions on Antennas and Propagation*, vol. 69, no. 6, pp. 3177-3192, June 2021.
15. X. Li, H. Zhou, Z. Gao, H. Wang and G. Lv, "Metamaterial Slabs Covered UWB Antipodal Vivaldi Antenna," in *IEEE Antennas and Wireless Propagation Letters*, vol. 16, pp. 2943-2946, 2017.
16. Guo, Minjie, et al. "High-gain antipodal Vivaldi antenna with metamaterial covers." *IET Microwaves, Antennas & Propagation* 13.15 (2019): 2654-2660.
17. Li X, Liu G, Zhang Y, Sang L, Lv G. A compact multi-layer phase correcting lens to improve directive radiation of Vivaldi antenna. *Int J RF Microw Comput Aided Eng.* 2017; 27:e21109.
18. X. X. Li, B. J. Lu, L. Sang, Y. M. Zhang, and G. Q. Lv, "Radiation enhanced Vivaldi antenna with shaped dielectric cover*," Microw. Opt. Technol. Lett*., vol. 59, no. 8, pp. 1975–1983, 2017.
19. Bhattacharjee, Anindita, et al. "Design of an antipodal Vivaldi antenna with fractal-shaped dielectric slab for enhanced radiation characteristics." *Microwave and Optical Technology Letters* 62.5 (2020): 2066-2074.
20. Xiangxiang Li, Dong Wei Pang, Hai Lin Wang, Yanmei Zhang, and Guoqiang Lv, "Dielectric Sheets Covered Broadband Vivaldi Antenna for Gain Enhancement," *Progress In Electromagnetics Research C*, Vol. 77, 69-80, 2017.
21. Tcvetkova, Svetlana N., et al. "Near-perfect conversion of a propagating plane wave into a surface wave using metasurfaces." *Physical Review B* 97.11 (2018): 115447.
22. W. Cao, W. Hong, Z. N. Chen, B. Zhang and A. Liu, "Gain Enhancement of Beam Scanning Substrate Integrated Waveguide Slot Array Antennas Using a Phase-Correcting Grating Cover," in *IEEE Transactions on Antennas and Propagation*, vol. 62, no. 9, pp. 4584-4591, Sept. 2014,
23. H. -R. Zu, B. Wu, Y. -T. Zhao, T. Su and Y. -F. Fan, "Dual-Band Antenna With Large Beam Steering Angle Incorporating Endfire and Frequency Scanning Modes Using Double-Layer SSPPs Structure," in *IEEE Transactions on Antennas and Propagation*, vol. 70, no. 1, pp. 46-55, Jan. 2022.
24. O. Yesilyurt and G. Turhan-Sayan, "Metasurface Lens for Ultra-Wideband Planar Antenna," in *IEEE Transactions on Antennas and Propagation*, vol. 68, no. 2, pp. 719-726, Feb. 2020.
25. Estakhri, Nasim Mohammadi, and Andrea Alu. "Wave-front transformation with gradient metasurfaces." *Physical Review* X 6.4 (2016): 041008.